RM E56K05a

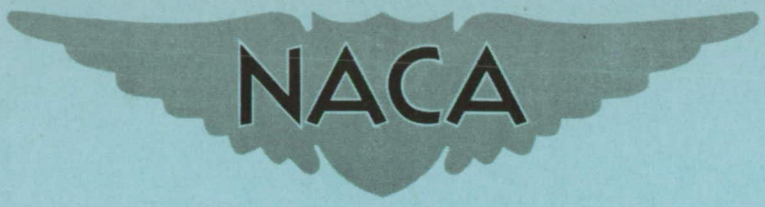

RESEARCH MEMORANDUM

EXPERIMENTAL EVALUATION OF METHODS FOR IMPROVING DIFFUSER-EXIT TOTAL-PRESSURE PROFILES FOR A SIDE-INLET MODEL AT MACH NUMBER 1.91

By John L. Klann

Lewis Flight Propulsion Laboratory
Cleveland, Ohio

NATIONAL ADVISORY COMMITTEE
FOR AERONAUTICS
WASHINGTON

January 22, 1957
Declassified December 3, 1958

NATIONAL ADVISORY COMMITTEE FOR AERONAUTICS

RESEARCH MEMORANDUM

EXPERIMENTAL EVALUATION OF METHODS FOR IMPROVING DIFFUSER-EXIT TOTAL-PRESSURE PROFILES FOR A SIDE-INLET MODEL AT MACH NUMBER 1.91

By John L. Klann

SUMMARY

A single cone side-inlet model was tested in the NACA Lewis 18- by 18-inch Mach number 1.91 wind tunnel. Total-pressure-distortion data were obtained for variations in constant-area mixing length at the end of the subsonic diffuser and inlet operation. Alterations to the basic configuration included: two cowl-lip bleed slots at the inlet floor, addition of uniform screens with systematic changes in mesh and flow-area blockage, and installation of a simulated compressor hub.

Data at a diffuser-exit Mach number of 0.36 are compared with data of a similar study at Mach 0.20. At the higher duct Mach number, the same length of natural mixing was less effective in reducing distortion, while screens were more effective. However, the greater effectiveness of screens at the high Mach number was accompanied by much larger total-pressure losses than occurred at the lower Mach number.

Direct results of this investigation showed that (1) reacceleration of the flow about the compressor hub was effective, within experimental limitations, in reducing distortion; and (2) for a given level of blockage, screens with small wire diameter and large mesh number resulted in the most rapid reduction of total-pressure distortion.

INTRODUCTION

The results of several natural and forced mixing devices are reported in reference 1 for a side-inlet model with a diffuser-exit Mach number of 0.20. All of these mixing schemes were successful in reducing total-pressure distortion at the compressor-face station. However, advanced engines are capable of operating at higher compressor-face Mach numbers. Therefore, in order to evaluate mixing devices at a higher discharge Mach number, several of the more favorable schemes of reference 1 were investigated in a side-inlet model with a diffuser-discharge Mach number of 0.36.

Distortion effects of the following model additions or changes were studied: (1) constant-area mixing lengths at the end of the subsonic diffuser, (2) screens with systematic variations in mesh and flow-area blockage, (3) bleed slots on the inlet cowl, and (4) a simulated compressor hub. The investigation was conducted in the NACA Lewis 18- by 18-inch Mach number 1.91 wind tunnel.

SYMBOLS

A flow area, sq in.

d diameter of constant-area duct, 2.20 in.

d_w diameter of screen wire, in.

l axial position of pressure rake in the constant-area duct (see fig. 1), in.

M Mach number

m mass flow

P total pressure

P_l total pressure at individual tube

ΔP maximum minus minimum value of total pressure at rake station

p static pressure

R radius of constant-area duct, 1.10 in.

r radial location of pressure tubes in rake, in.

ϵ number of wires per inch of screen

Θ angular location of throat survey tubes (see fig. 3), deg

φ screen solidity (or flow-area blockage)

Subscripts:

th throat

0 free stream

1 conditions at model station 0

2 conditions at movable pressure rake

3 conditions at mass-flow measuring station

Superscript:

$\bar{}$ arithmetic average

APPARATUS AND PROCEDURE

Details of the model are shown in figure 1. A half-conical external compression surface, positioned to provide approximately 10-percent spillage at the inlet lip for a free-stream Mach number of 1.91, was followed by the subsonic-diffuser flow-area variation shown in figure 2. The constant-area section indicated in figures 1 and 2 was 3.5 diffuser-exit diameters long. Instrumentation in this part of the model included a pressure rake in the constant-area duct and a set of rakes at model station 0. This latter set of rakes, which consisted of 21 total-pressure tubes placed in three circumferential arrays of seven tubes each, was installed in the model for only part of the test program.

Details of the constant-area pressure rake are also shown in figure 1. For one series of tests, a simulated compressor hub was seated over the nine innermost total-pressure tubes of this rake. The ratio of the hub radius to the duct radius was 0.500. With or without the presence of this hub, the rake total-pressure tubes were located (with the exception of the center tube) at the centroids of equal areas. The rake, or rake and hub combination, was remotely translated through the length of the constant-area passage. Data from this rake were used in calculating average inlet total-pressure recovery $\bar{P}_2/P_0$ and distortion $\Delta P_2/\bar{P}_2$.

The remaining portion of the model (not shown in fig. 1) was exactly as reported in reference 1. Downstream of model station 18.18, the captured air was further diffused to another constant-area duct where the model airflow was regulated with an exit plug. Four wall static-pressure orifices in this duct were used in conjunction with the plug exit area in calculations of inlet mass flow.

Modifications to the basic configuration included (1) the addition of two cowl-lip bleed slots at the diffuser floor (one is shown in fig. 1), and (2) the installation of a series of uniform screens at model station 10.49. The screen series first varied flow-area blockage at a constant mesh ($\epsilon = 2$) and then mesh at a constant blockage ($\varphi = 0.19$). Dimensions and values of parameters for these screens are presented in table I.

The investigation was conducted in the NACA Lewis 18- by 18-inch Mach number 1.91 wind tunnel. Total temperature and dewpoint were maintained at 150° and -5° F (or less), respectively, while tunnel total pressure was approximately atmospheric. The model was mounted in the tunnel as a nose inlet.

Two of the basic model modifications were tested with a series of the screens: (1) the model with the cowl bleed addition and no diffuser reacceleration, and (2) the model with compressor-hub reacceleration and no bleed. Tests without diffuser screens were conducted with (1) the basic configuration, (2) basic with bleed, and (3) basic with compressor hub.

Distortion and pressure-recovery data were taken at four longitudinal positions of the pressure rake in the duct. With the model alined to the tunnel axis, these data were obtained over a mass-flow range for all configurations.

RESULTS AND DISCUSSION

The effect of the addition of cowl-lip bleed slots on the total-pressure distributions at the inlet (model station 0) is shown in figure 3. For the basic inlet, the lowest-energy air occurred near the corners formed by the centerbody surface and splitter-plate floor. The use of lip bleed did not significantly reduce the distortion parameter $\Delta P/\overline{P}$, defined as the maximum minus the minimum total pressure at any measuring station divided by the average total pressure at that station. On the other hand, the average pressure recovery was reduced a small amount. In general, therefore, the lip-bleed system was not effective in improving inlet performance.

In the following sections, diffuser-exit data are presented and discussed under the two groupings, "Basic Model" and "Model with Compressor Hub." Average pressure-recovery and distortion data obtained at the diffuser exit are summarized in table II. The higher pressure recovery for the model with compressor hub, which may be noted in table II, will be discussed later.

Basic Model

The basic configuration was tested with and without the bleed slots and with bleed and the constant-mesh screen series. Inlet performance curves are presented in figure 4. These pressure-recovery curves were identical for all positions of the pressure rake in the constant-area passage. Hence, only data points for a nondimensional distance l/d of 0.19 are indicated. The associated distortion-number variations with mass flow in figure 4 were typical in form but different in magnitude from those obtained at other positions of the pressure rake.

Typical total-pressure profiles for the case without bleed or screens are presented in figure 5 for a range of mass flow. Contours are expressed as the percent above or below the average total pressure measured at the rake. The average values of the four static pressures (see fig. 1) measured at the rake are also presented as the percent below the average total pressure. In addition, mass-flow ratio, average total-pressure recovery, and distortion number are indicated for each profile. The distortion numbers are expressed to three decimal places, whereas the contours are labeled to the nearest percent. Hence, the difference between the maximum and minimum contour values is only approximately equal to the distortion number. In general, the higher pressure cores were located in the upper portion of the duct. Also, in each of these profiles, high and low regions of nearly the same magnitude were present; hence, each zero contour encloses approximately half of the duct area.

For a measure of effectiveness in reducing distortions, turbulent pipe-flow distortion values are plotted in figure 6 as a function of average duct Mach number. The values were calculated to 0.934 of the duct radius for a 1/7-power velocity profile. This radius ratio, 0.934, corresponds to the physical location of the outermost pressure tube in the translating rake. Reference 2 has shown that these pipe-flow values show distortion trends and that they may be considered as reference distortions or limiting values. For example, a rise in distortion with increasing duct Mach number is shown in figure 6. The same trend is seen in figure 4. The more abrupt experimental rise was probably due to internal-shock - boundary-layer interactions, which cause local flow separations, as pointed out for similar cases in references 2 and 3.

Total-pressure distortion numbers are plotted against the constant-area mixing-length parameter l/d in figure 7 for a diffuser-exit Mach number of 0.36. For all configurations, distortion decreased with increased mixing length. The addition of bleed slots at the inlet cowl caused very little change in the distortion characteristics with respect to mixing length (fig. 7(a)).

The effect of uniform screens (placed at an l/d of zero) on the distortion variations is shown in figure 7(b). After 2 diameters of mixing length, distortion decreased with increased blockage, the largest reduction due to screens occurring after the complete length of mixing (3.5d). Figure 6 shows that the pipe-flow reference value of distortion at an average duct Mach number of 0.36 is 0.076. The data for mixing after the screen with 0.30 blockage are most nearly approaching this value. Hence, in this case, the use of screens in conjunction with natural mixing lengths might be thought of as accelerating the natural mixing process.

The effect of screens on the total-pressure profiles is presented in figure 8. The high pressure cores are still located in the top half of the duct passage, while the pressure distributions again have equally high and low regions for screen blockages φ of 0.19 and 0.30.

Figure 9 shows the percent loss in total pressure across screens as a function of flow-area blockage for the present data at a duct Mach number of 0.36 and for similar data from reference 1 at a Mach number of 0.20. The data from reference 1 have also been used to predict the losses at Mach 0.36 from the assumption that the losses are directly proportional to the entering dynamic pressure. The experimental curve shows slightly larger losses; however, the estimate is a good first approximation. Figure 10 shows the associated reductions in distortions measured at l/d of 3.5 by varying the flow-area blockage. It should be noted that in this figure the no-screen distortions for Mach 0.36 and 0.20 are 0.157 and 0.044, respectively. Figures 9 and 10 show that, for the same percentage reduction in distortion, the total-pressure losses across the screens at the higher Mach number were 1.5 to 2 times the losses at Mach 0.20.

Model with Compressor Hub

The configuration with the simulated compressor hub was tested without the lip-bleed addition but with the constant-mesh and constant-blockage screen series. Inlet performance curves are presented in figure 11. Supercritical data were limited because of choking at the rake, which was caused by the area reduction of the hub in combination with the total-pressure losses across the screens. As in the previous results, no change in recovery occurred with mixing length; and, therefore, only the data points for the first measuring stations in the constant-area duct are shown. With the addition of screens, the first measuring station was changed from l/d of 0.19 to 0.58.

Distortion numbers are plotted against constant-area mixing-length in figure 12 for a Mach number of 0.52. This Mach number over the compressor hub corresponds to a Mach number of 0.36 in the basic flow passage. The constant-mesh screen distributions of figure 12(a) show that, after 1 diameter of mixing, distortions decreased with increased flow-area blockage. In general, the largest improvements in distortion occurred at the end of the mixing section.

The effect of mesh is shown in the constant-blockage curves of figure 12(b). The larger-mesh screens (ϵ = 4 and 6) were more effective in the first 1.5 diameters of mixing. This figure also shows that the additional mixing lengths beyond 2 diameters for ϵ of 4 and 6 slightly increased the measured distortion level. Within experimental accuracy, the total-pressure losses across these screens were the same as those shown in figure 9.

The constant-blockage data of figure 12(b) are replotted in figure 13 as a function of a different nondimensional mixing-length parameter l/d_w, the axial distance in the constant-area duct divided by the diameter of the screen wire. An optimum value of l/d_w of about 150 existed

for the screen configurations investigated. Higher values did not markedly increase the resultant distortion, however. As l/d_w decreased below 150, the distortion increased rapidly, probably because of large wakes from the screen wires which impinged on the measuring tubes. In general, these data indicate the desirability of using screens having large mesh numbers and small wire diameters to achieve the most rapid distortion reduction with a given screen blockage.

Sample total-pressure profiles with and without screens are presented in figure 14. The higher-energy air that existed in the top half of the duct without the simulated hub (see fig. 8) was displaced to the upper surface of the compressor hub. Comparisons with analogous profiles without the hub (fig. 8) show that some high- or low-energy air, or both, measured without the hub, was not picked up by the reduced instrumentation. Because of the acceleration of the compressor hub, the low-energy stream tubes of the basic flow passage have been displaced closer to the walls of the annular passage. Hence, this different measuring technique can also explain the higher level of average total-pressure recovery shown in table II for the model with the compressor hub.

Distortion values obtained without screens are presented in figure 15 as a function of straight mixing length for the duct Mach numbers of the present investigation and of reference 1. Natural mixing was much more effective at the duct Mach number of 0.20 than at Mach 0.36. The distortion levels at the entrance to the straight mixing length differed; however, distortion dropped about 72 percent over the 3.5-diameter passage length for Mach number 0.20, compared with 15 percent for Mach 0.36. This greater effectiveness of natural mixing at the lower Mach number would be expected from the longer residence time and higher shear of the lower-speed flow. The distortions at Mach 0.36 showed no tendency to approach the pipe-flow value of 0.076 (from fig. 6). On the other hand, the Mach 0.20 flow was rapidly approaching its pipe-flow value of 0.022.

Turning to a comparison of the Mach 0.36 and 0.52 curves of figure 15, a substantial distortion reduction is shown for Mach 0.52. Because of the reduced instrumentation with the compressor hub and the noted displacement of the low-energy stream tubes closer to the outer wall of the annular passage, the exact value of the real reduction in distortion is not known. However, within these limitations, the compressor hub did reduce total-pressure distortion.

CONCLUSIONS

Investigation of methods for improving total-pressure distortions at a diffuser-exit Mach number of 0.36 and comparisons with similar data at Mach number 0.20 indicated the following:

1. The same length of natural mixing in constant-area ducts following subsonic diffusers was less effective in reducing distortions at the higher Mach number.

2. Reacceleration of inlet flow about a simulated compressor hub was effective, within experimental limitations, in reducing distortions.

3. Increasing flow-area blockage by the use of uniform screens resulted in larger distortion reductions at the higher Mach number. However, for the same percentage reduction in distortion, the total-pressure losses across the screens at the higher Mach number were from 1.5 to 2 times the losses at Mach 0.20.

4. For a given level of blockage, screens with small wire diameter and large mesh number gave the most rapid reduction in distortion.

Lewis Flight Propulsion Laboratory
National Advisory Committee for Aeronautics
Cleveland, Ohio, November 6, 1956

REFERENCES

1. Piercy, Thomas G., and Klann, John L.: Experimental Investigation of Methods of Improving Diffuser-Exit Total-Pressure Profiles for a Side-Inlet Model at Mach Number 3.05. NACA RM E55F24, 1955.

2. Sterbentz, William H.: Factors Controlling Air-Inlet Flow Distortions. NACA RM E56A30, 1956.

3. Piercy, Thomas G.: Factors Affecting Flow Distortions Produced by Supersonic Inlets. NACA RM E55L19, 1956.

TABLE I. - SCREEN PARAMETERS

Number of wires per inch, ϵ	Wire diameter, d_w, in.	Screen solidity, φ
2	0.0260	0.101
2	.0508	.193
4	.0253	.192
5.5	.0179	.187
2	.0808	.297

TABLE II. - SUMMARY OF PRESSURE-RECOVERY AND DISTORTION DATA

Model	Screens at model station 10.49		Average rake Mach number, $\bar{M}_2$	Average total-pressure recovery, $\bar{P}_2/P_0$	Distortion number at l/d of 3.47, $\Delta P_2/\bar{P}_2$
	φ	ϵ			
Basic	0	0	0.36	0.881	0.172
Basic with lip bleed	0	0	0.36	0.859	0.157
	.10	2		.851	.129
	.19	2		.837	.097
	.30	2		.808	.083
Basic with compressor hub	0	0	0.52	0.903	0.132
	.10	2		.894	.100
	.19	2		.868	.081
	.19	4		.880	.088
	.19	6		.878	.099
	.30	2		.838	.062

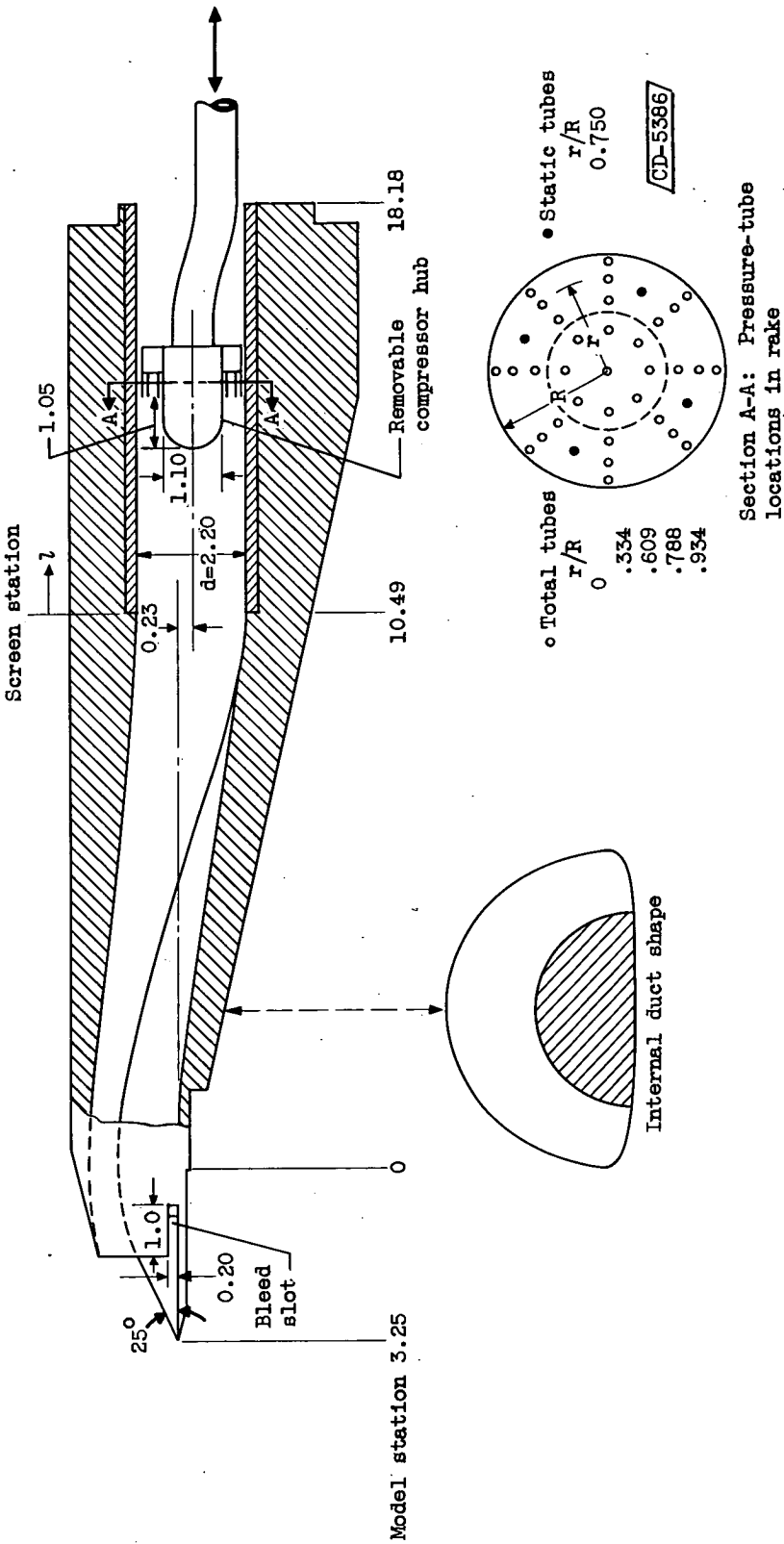

Figure 1. - Model details (dimensions in inches).

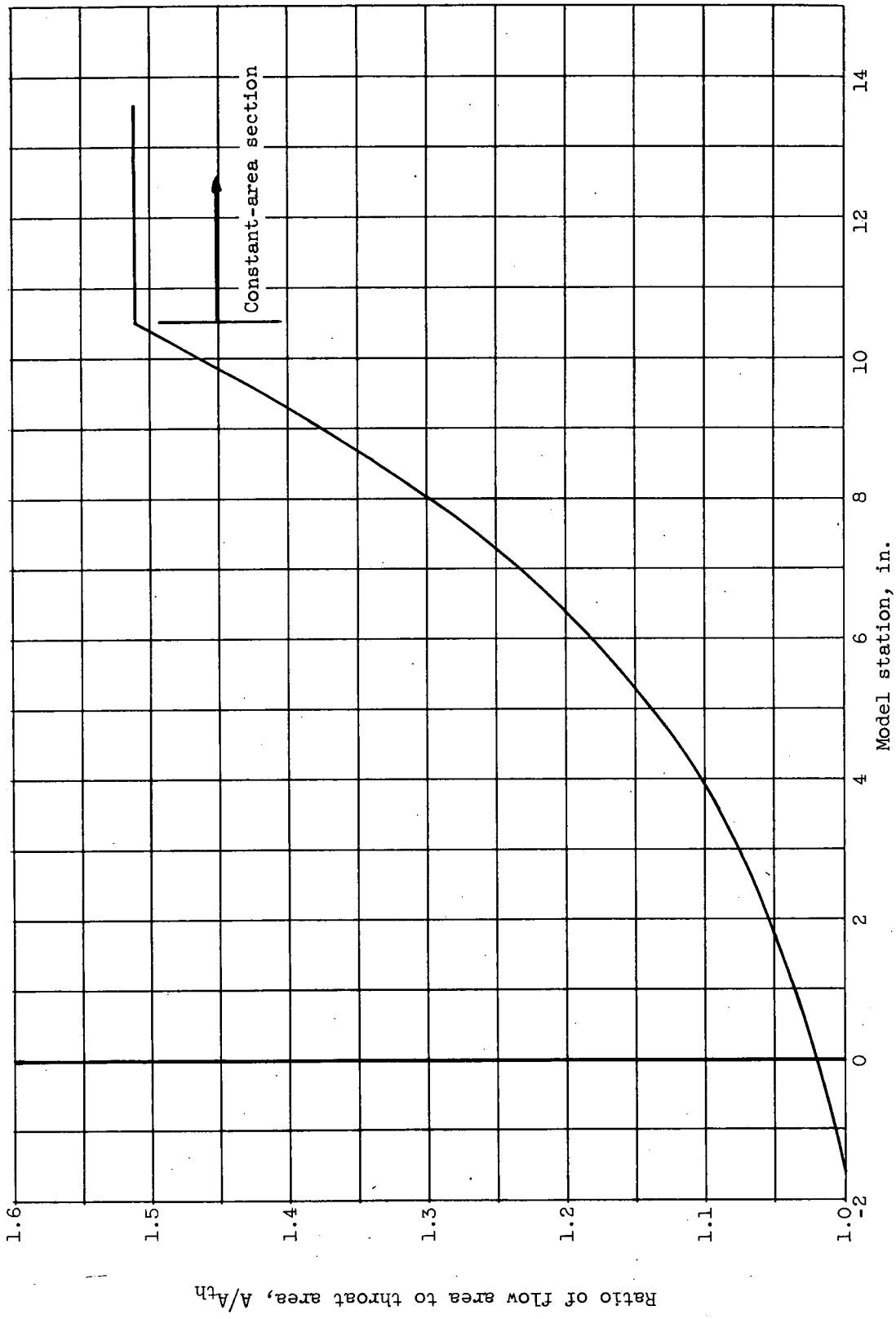

Figure 2. - Subsonic-diffuser area variation.

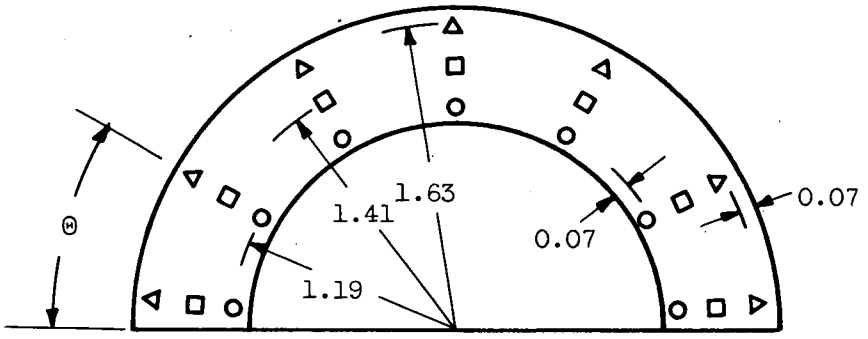

Location of survey tubes

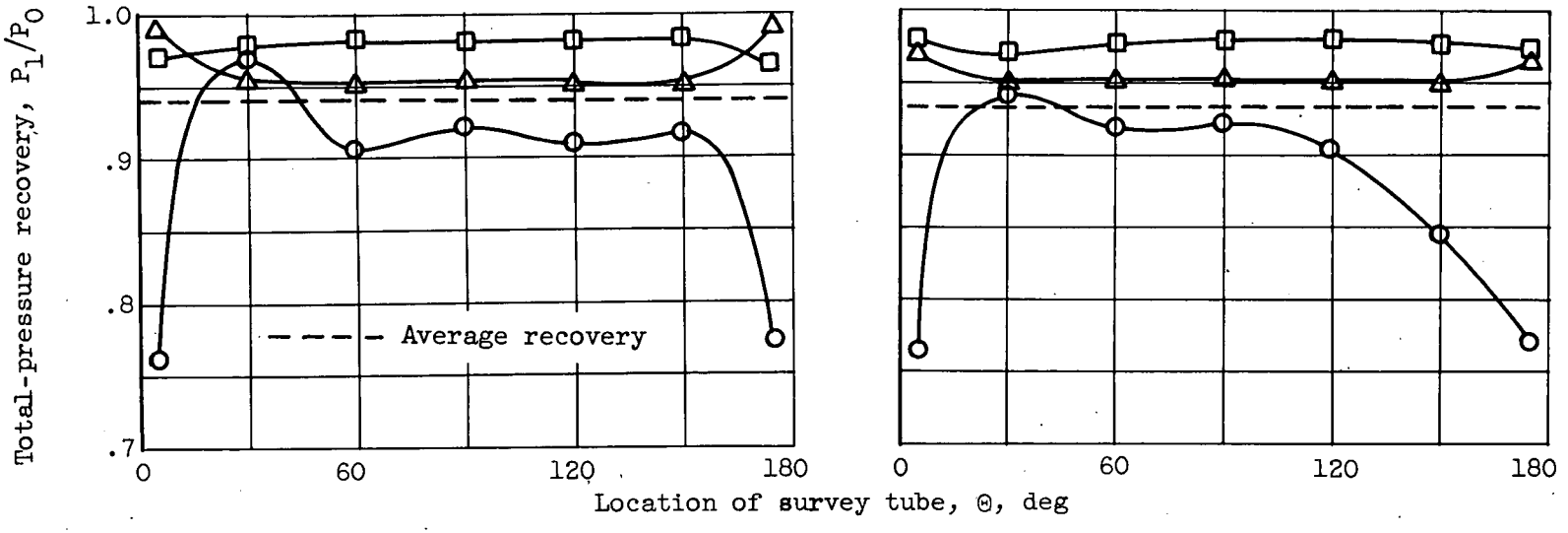

(a) Basic configuration. Distortion number $\Delta P_1/\overline{P}_1$, 0.245.

(b) Lip-bleed configuration. Distortion number $\Delta P_1/\overline{P}_1$, 0.232.

Figure 3. - Inlet surveys at model station 0 (dimensions in inches).

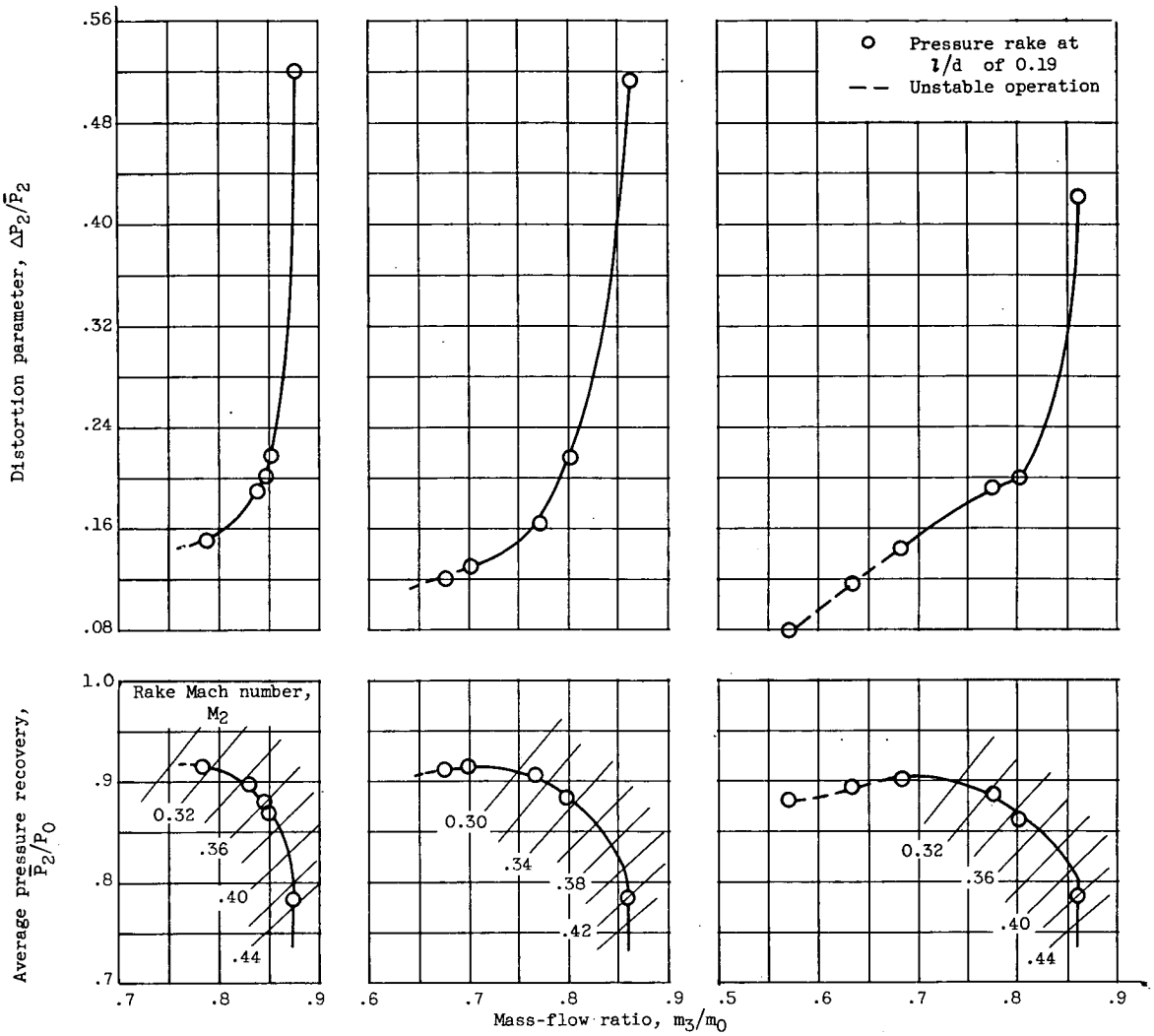

(a) Screen blockage φ, 0; no bleed.

(b) Screen blockage φ, 0; lip bleed.

(c) Screen blockage φ, 0.10; screen mesh ε, 2; lip bleed.

Figure 4. - Inlet performance curves. Effect of lip bleed and screens.

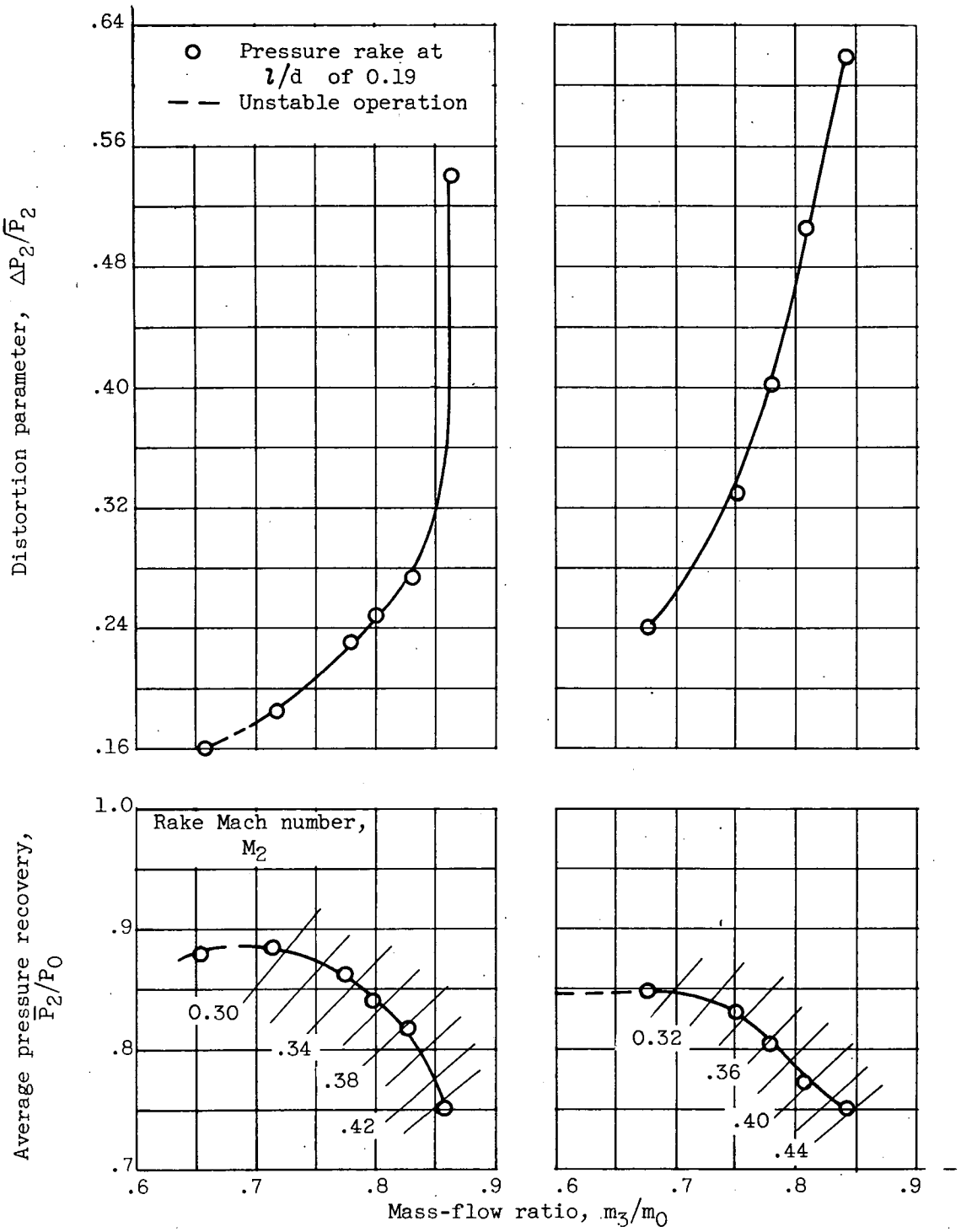

(d) Screen blockage φ, 0.19; Screen mesh ε, 2; lip bleed.

(e) Screen blockage φ, 0.30; screen mesh ε, 2; lip bleed.

Figure 4. - Concluded. Inlet performance curves. Effect of lip bleed and screens.

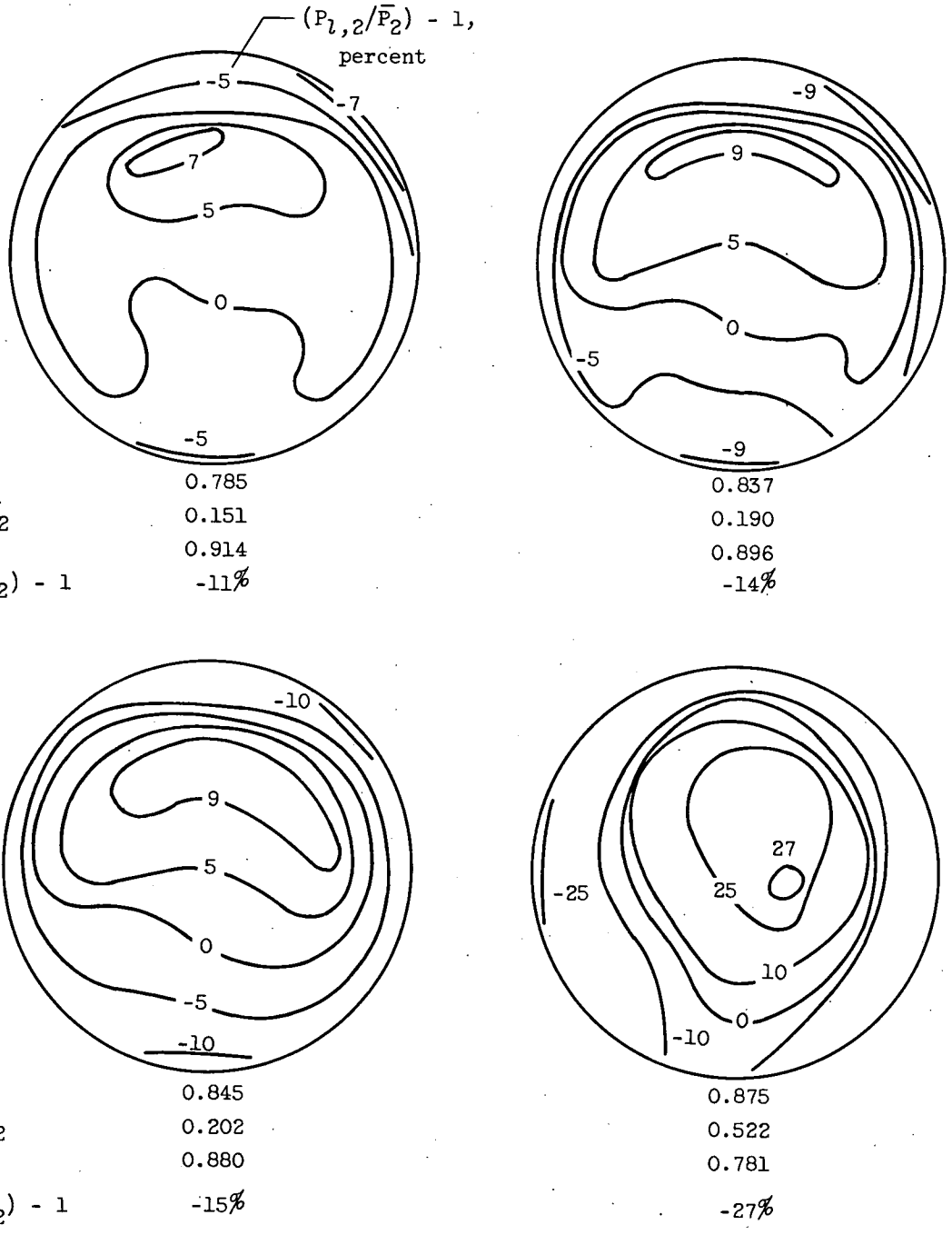

m_3/m_0	0.785	0.837
$\Delta P_2/\bar{P}_2$	0.151	0.190
$\bar{P}_2/P_0$	0.914	0.896
$(\bar{p}_2/\bar{P}_2) - 1$	-11%	-14%
m_3/m_0	0.845	0.875
$\Delta P_2/\bar{P}_2$	0.202	0.522
$\bar{P}_2/P_0$	0.880	0.781
$(\bar{p}_2/\bar{P}_2) - 1$	-15%	-27%

Figure 5. - Variation of total-pressure profiles. Effect of mass flow. Mixing length l/d, 0.19; screen blockage ϕ, 0; no bleed.

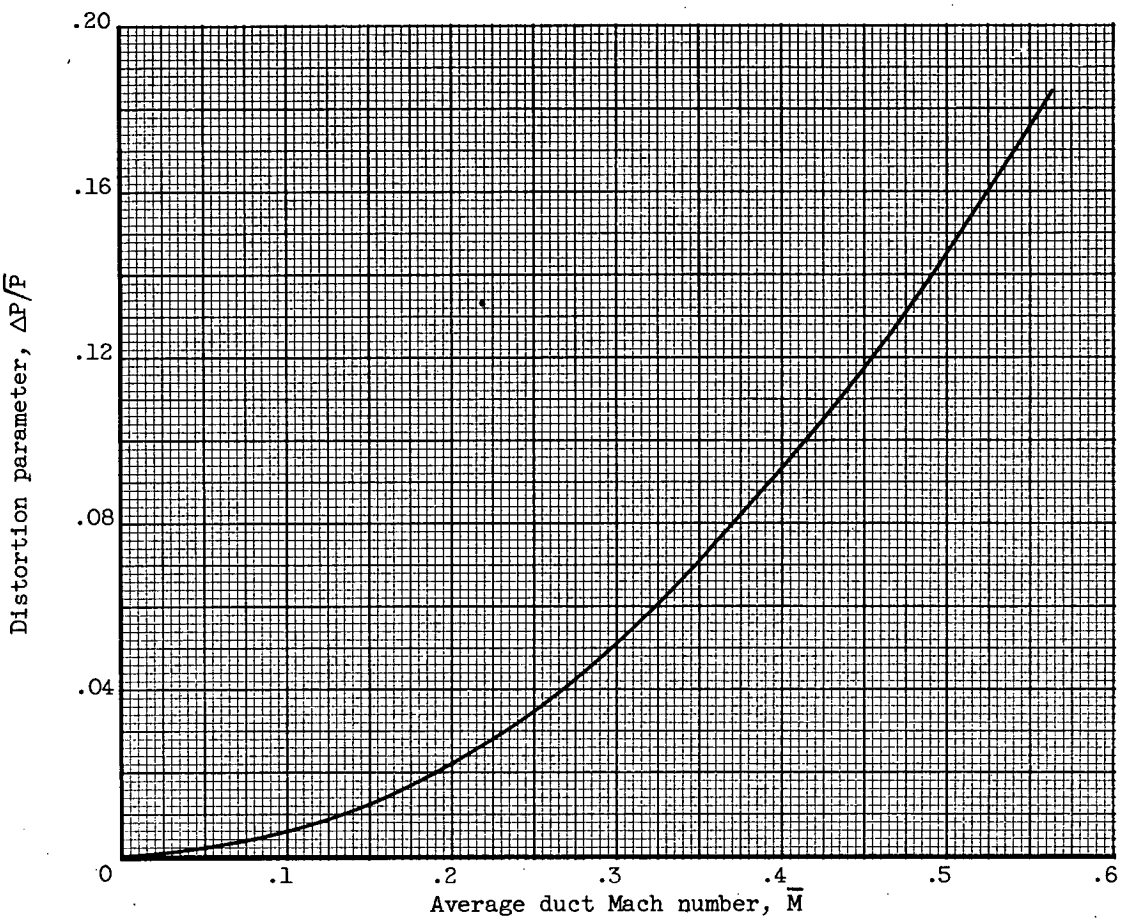

Figure 6. - Total-pressure distortion for a three-dimensional, 1/7-power velocity profile to a radius ratio of 0.934.

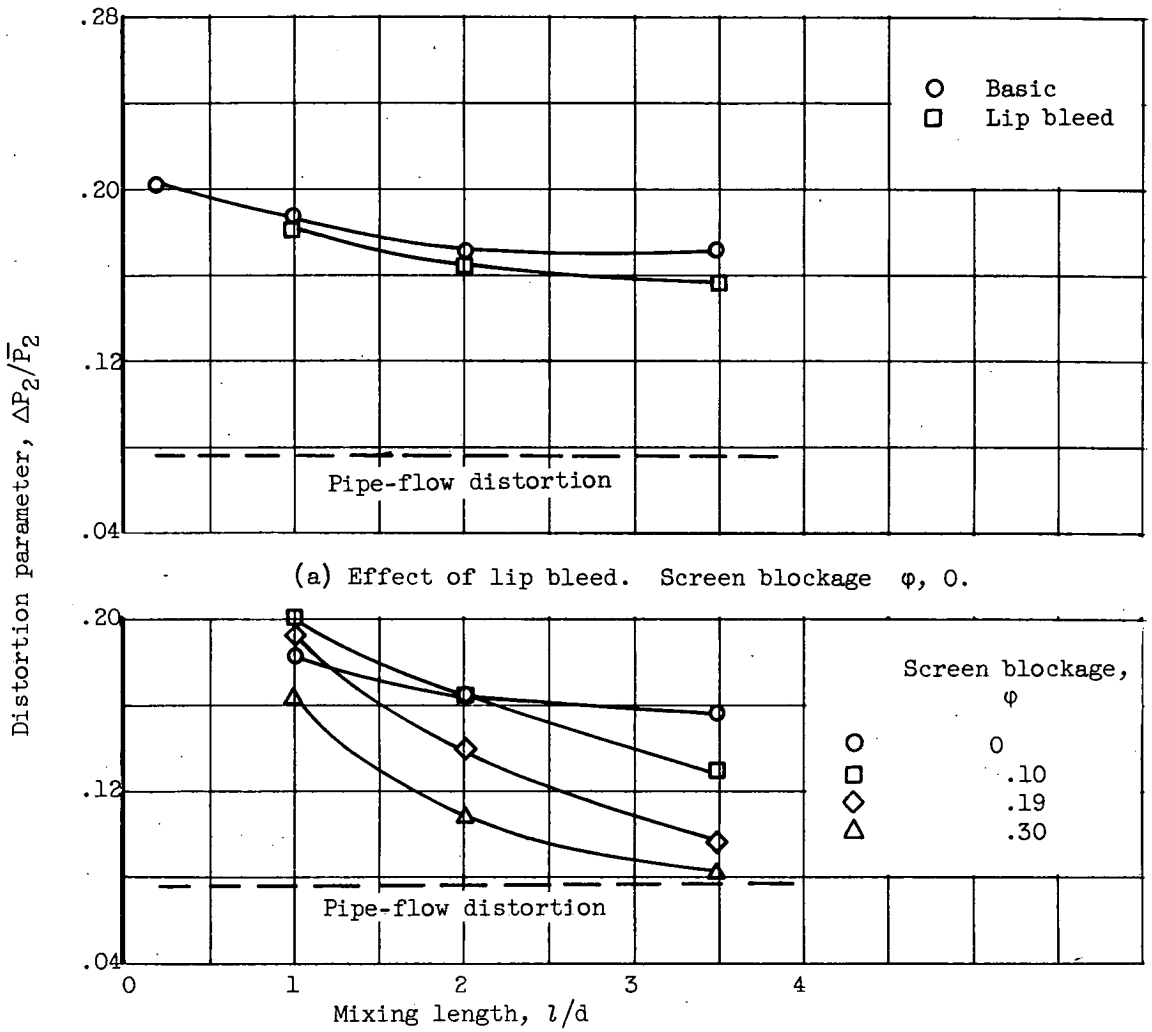

(a) Effect of lip bleed. Screen blockage φ, 0.

(b) Effect of screen blockage with lip bleed. Screen mesh ε, 2.

Figure 7. - Variation of total-pressure distortion in diffuser constant-area section with mixing length. Average Mach number, 0.36.

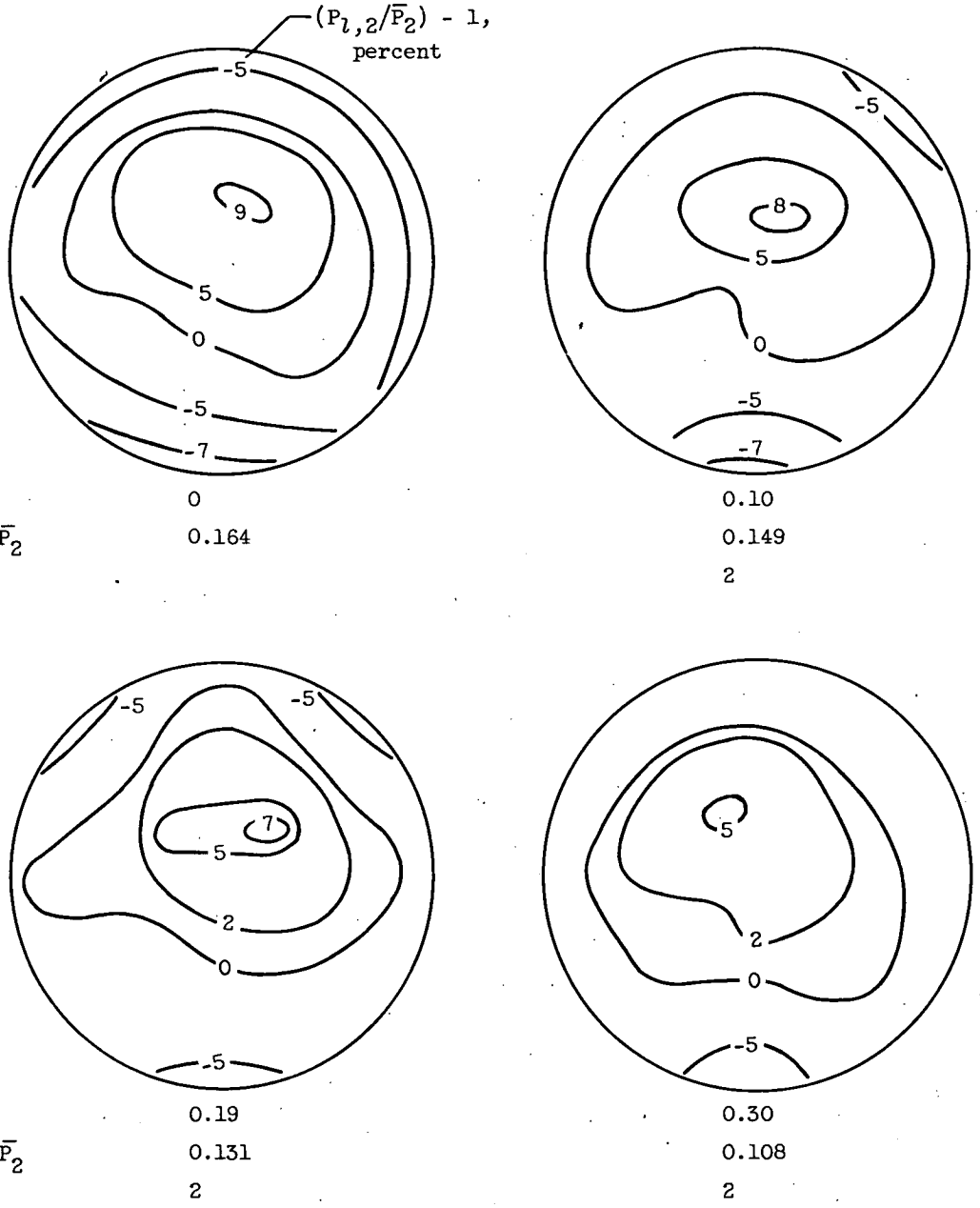

φ	0	0.10
$\Delta P_2/\bar{P}_2$	0.164	0.149
ε		2

φ	0.19	0.30
$\Delta P_2/\bar{P}_2$	0.131	0.108
ε	2	2

Figure 8. - Variation of total-pressure profiles. Effect of lip bleed and screen blockage. Mixing length l/d, 2.00; average Mach number, 0.36; average rake static pressure $(\bar{p}_2/\bar{P}_2)$ - 1, -14 percent; lip bleed.

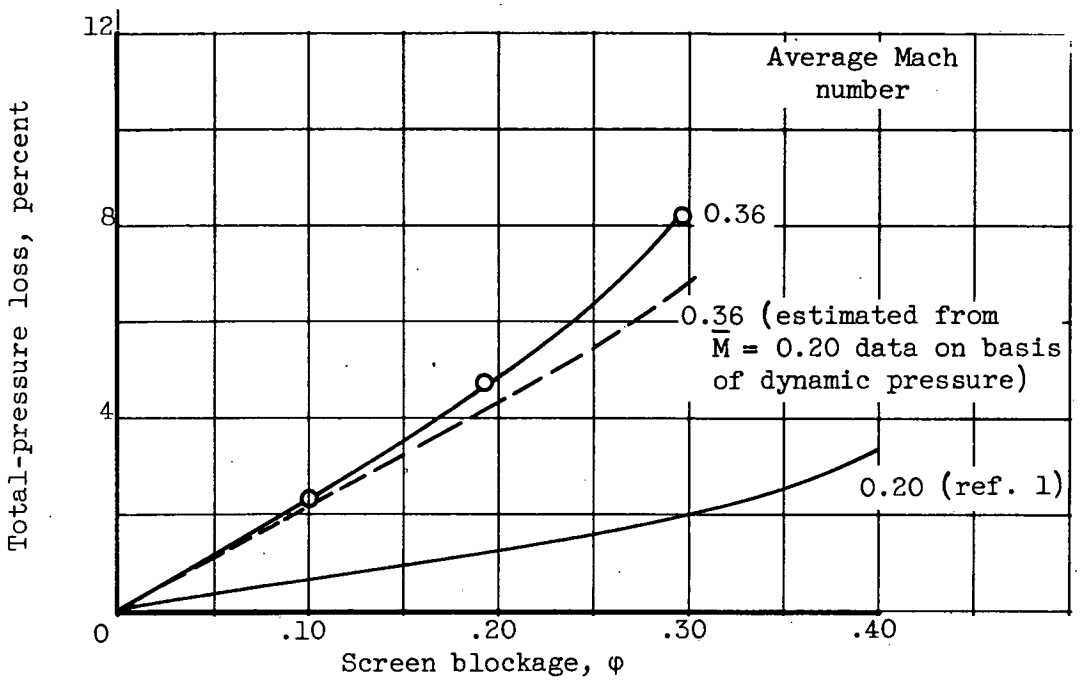

Figure 9. - Total-pressure losses with screens.

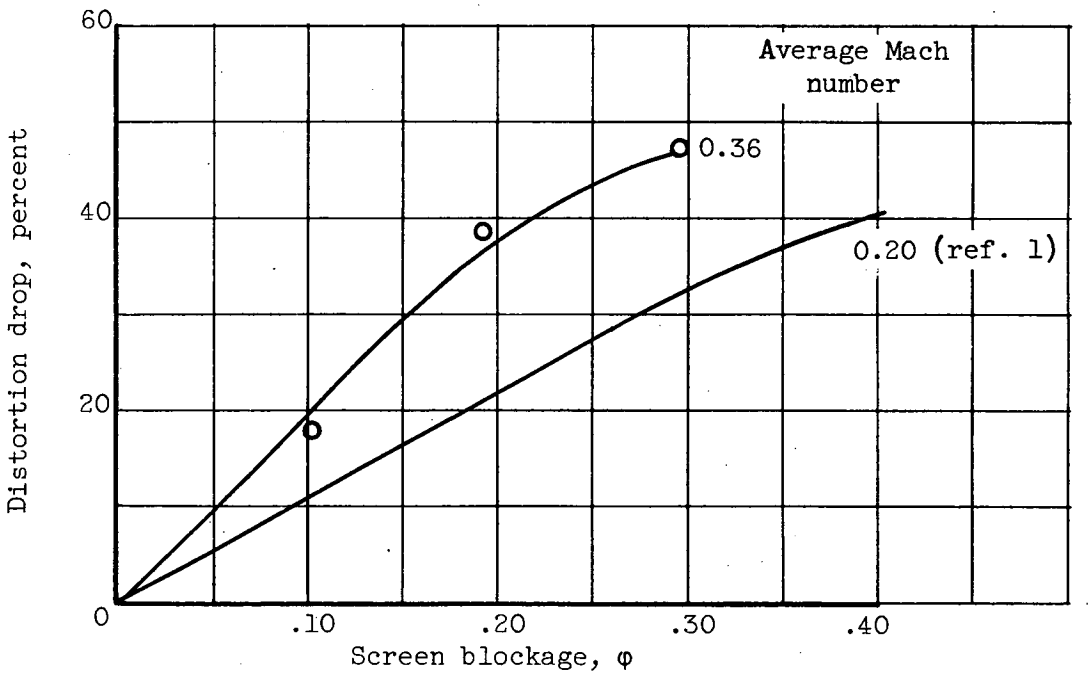

Figure 10. - Distortion reduction with screens. Mixing length l/d, 3.5.

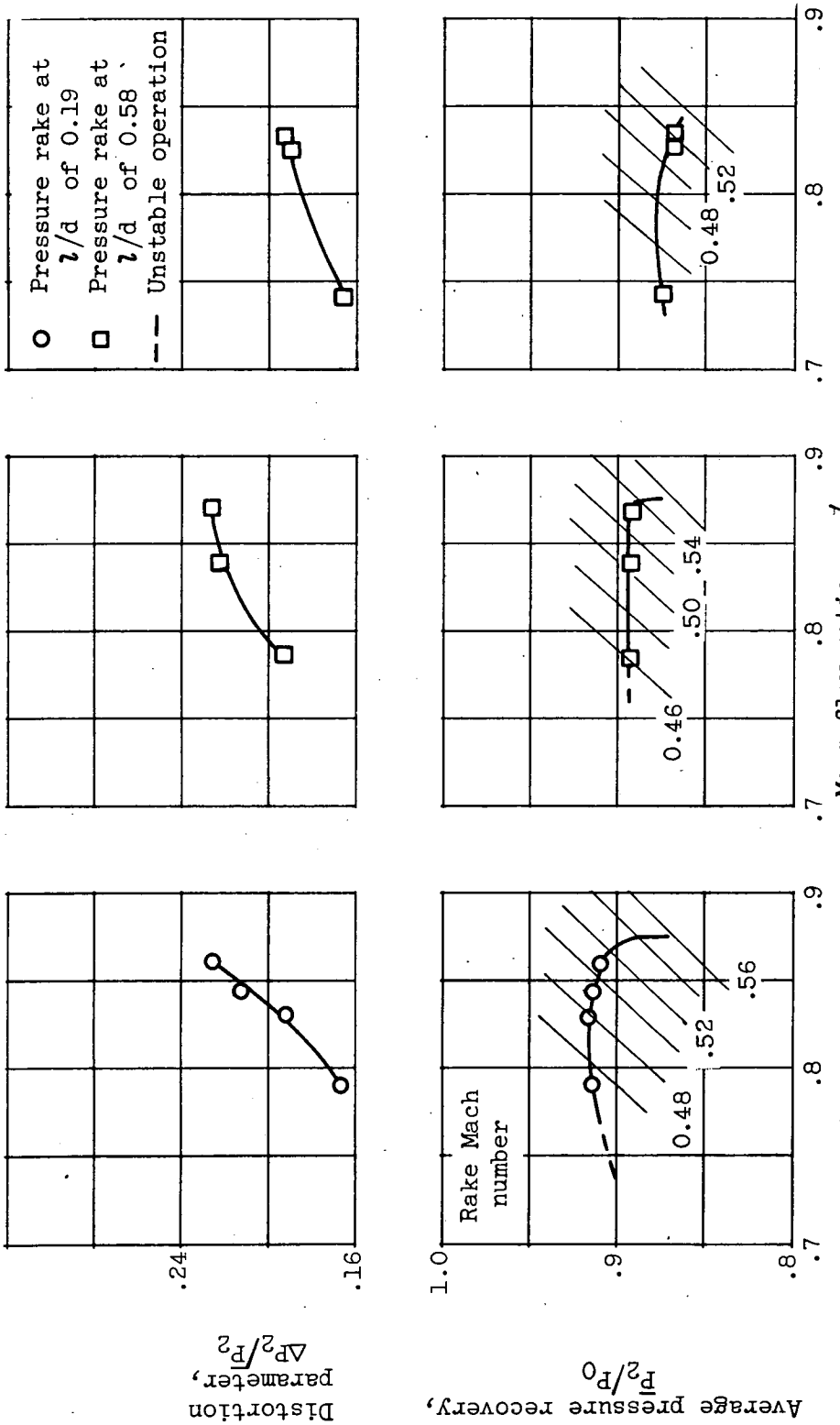

(a) Screen blockage φ, 0.

(b) Screen blockage φ, 0.10 screen mesh ϵ, 2.

(c) Screen blockage φ, 0.19; screen mesh ϵ, 2.

Figure 11. - Inlet performance curves with compressor hub. Effect of screens.

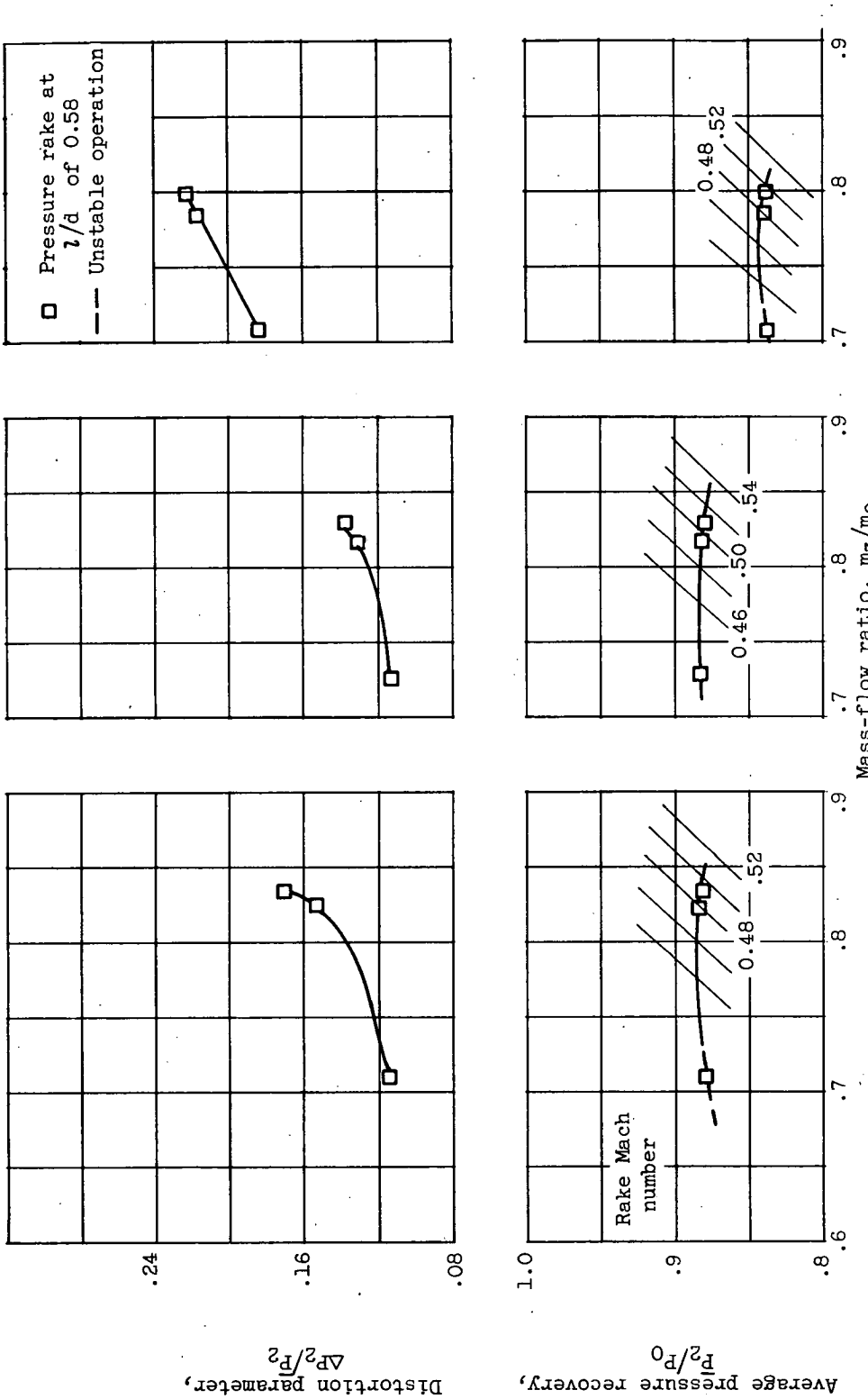

(d) Screen blockage φ, 0.19; screen mesh ε, 4.

(e) Screen blockage φ, 0.19; screen mesh ε, 6.

(f) Screen blockage φ, 0.30; screen mesh ε, 2.

Figure 11. - Concluded. Inlet performance curves with compressor hub. Effect of screens.

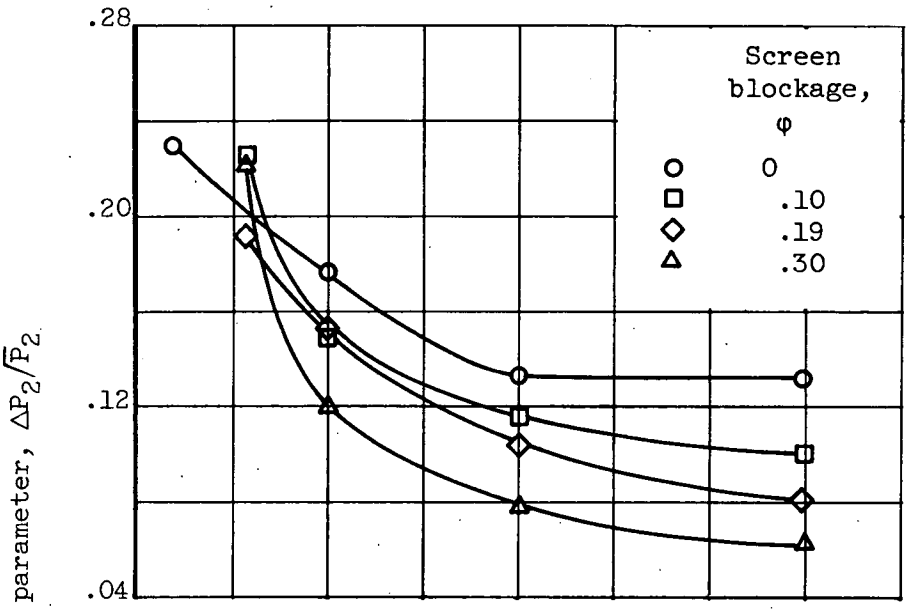

(a) Effect of screen blockage. Screen mesh ε, 2.

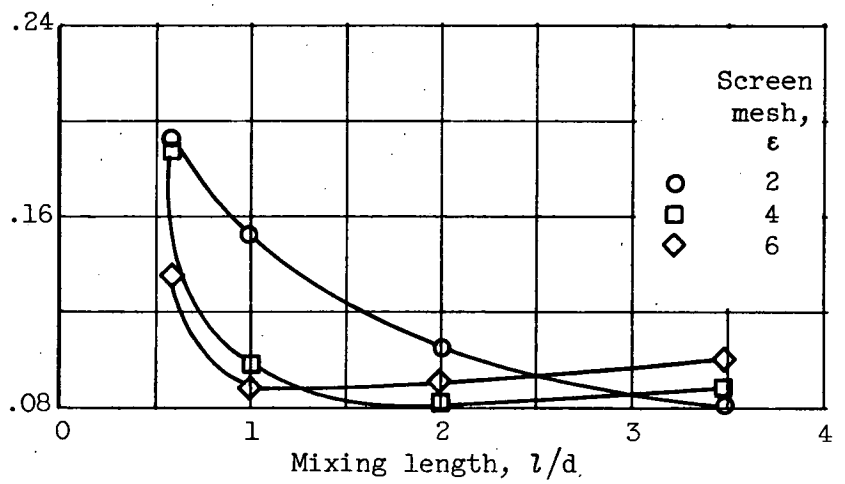

(b) Effect of screen mesh. Screen blockage φ, 0.19.

Figure 12. - Variation of total-pressure distortions at compressor hub with constant-area mixing length. Average hub Mach number, 0.52.

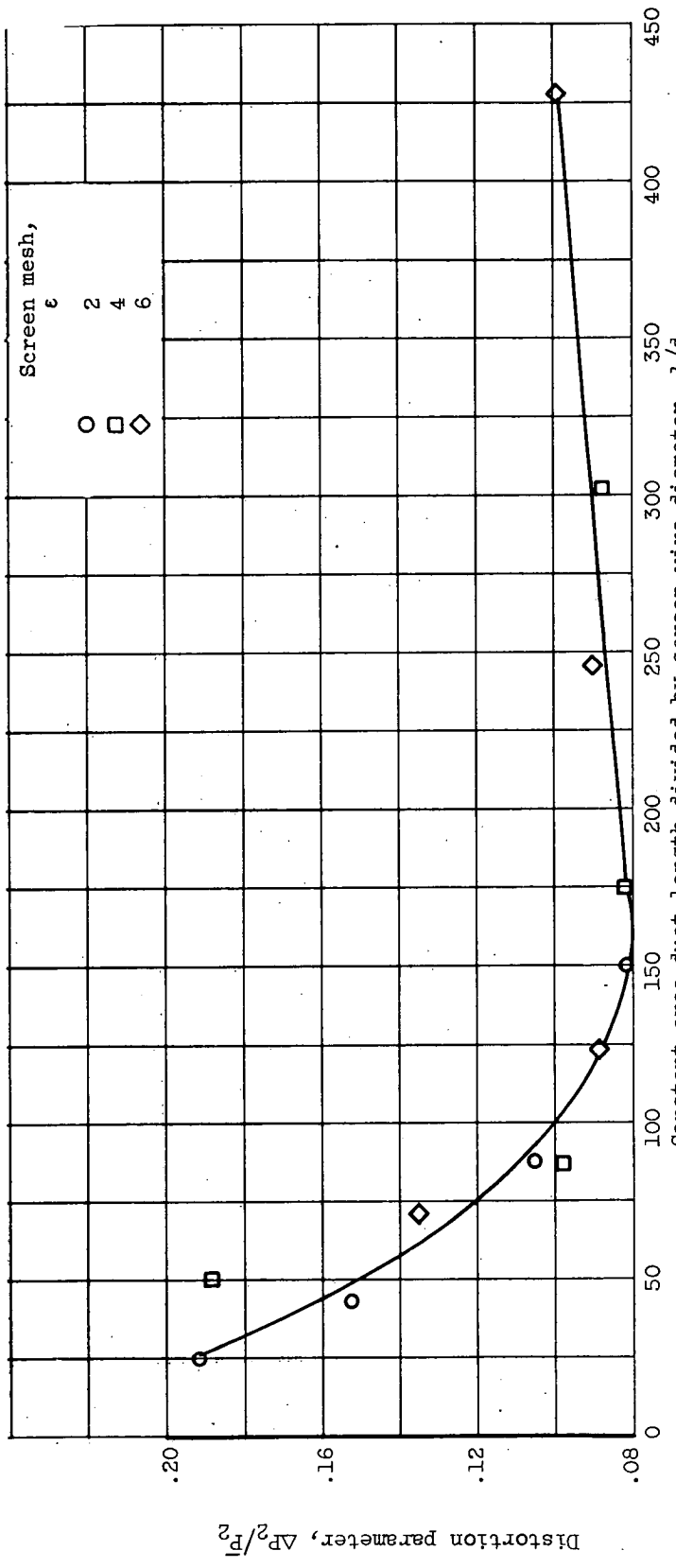

Figure 13. - Screen-mesh effect at constant blockage of 0.19. Average hub Mach number, 0.52.

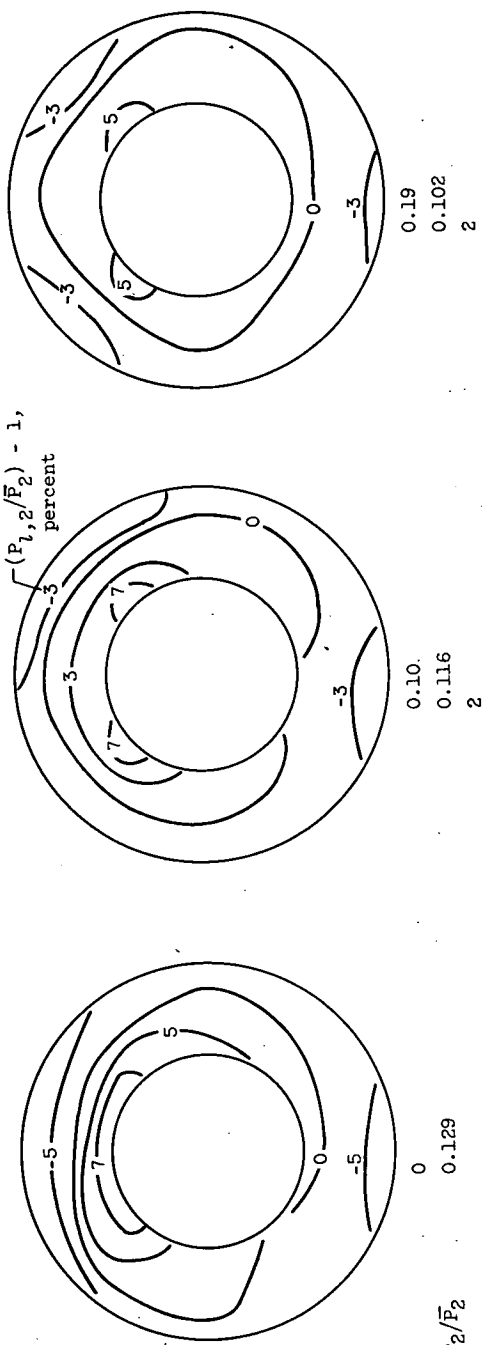

Figure 14. - Variation of total-pressure profiles. Effect of screens. Mixing length l/d, 2.00; average hub Mach number, 0.52; $(\bar{P}_2/\bar{P}_2 - 1) = -24$ percent for each profile.

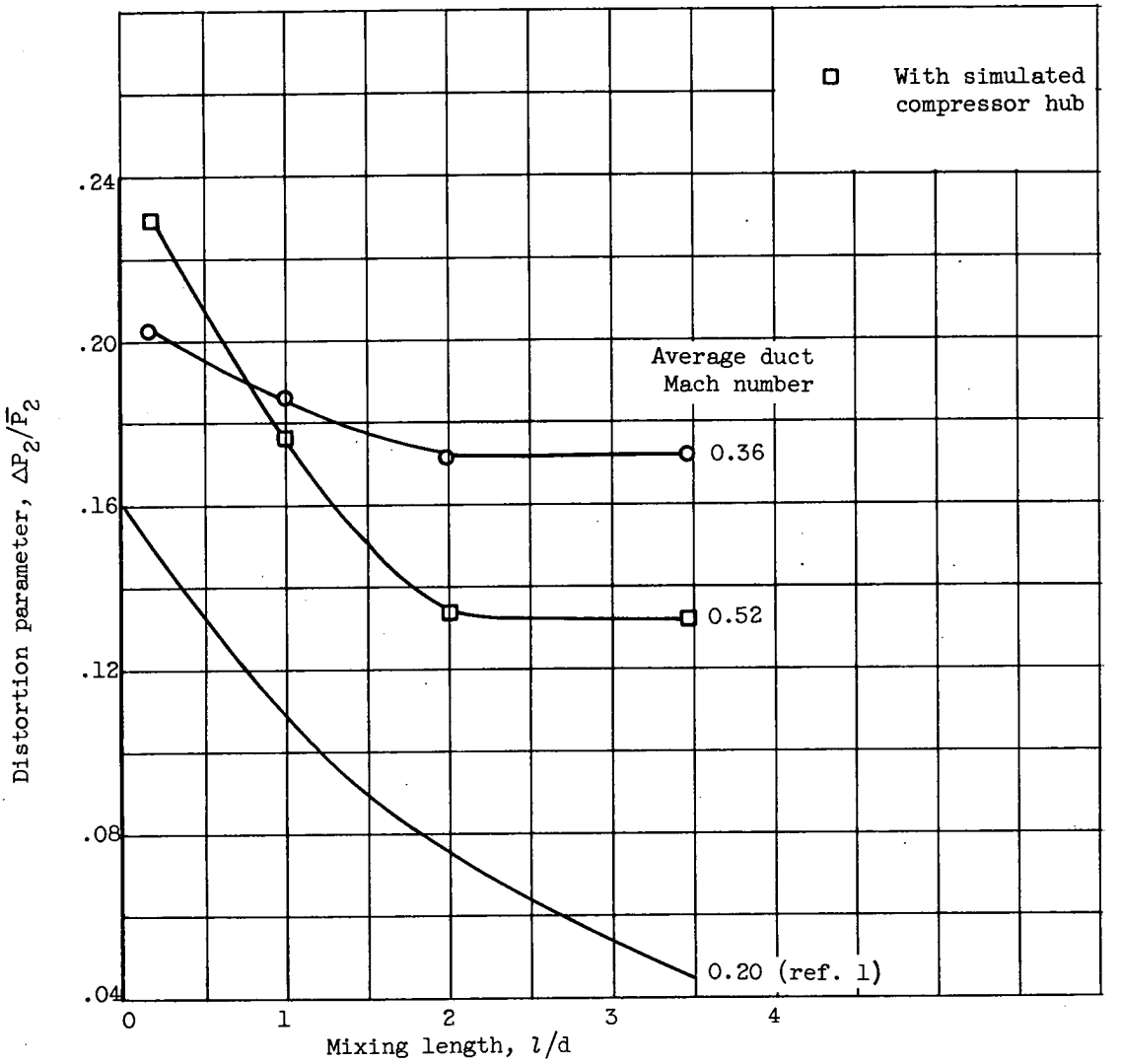

Figure 15. - Effect of duct Mach number on distortion.